ChemComm

Photochromic dinuclear iridium(III) complexes having phenoxyl-imidazolyl radical complex derivatives

Journal:	*ChemComm*
Manuscript ID	CC-COM-05-2023-002208.R1
Article Type:	Communication

ChemComm

COMMUNICATION

Photochromic dinuclear iridium(III) complexes having phenoxyl-imidazolyl radical complex derivatives

Received 00th January 20xx,
Accepted 00th January 20xx

DOI: 10.1039/x0xx00000x

www.rsc.org/

Yoshinori Okayasu,[a] Takuya Miyahara,[a] Rintaro Shimada,[b] Yuki Nagai,[a] Akira Sakamoto,[b] Jiro Abe*[b] and Yoichi Kobayashi*[a,c]

We demonstrate that phenoxyl-imidazolyl radical complex (PIC), which is a rate-tunable fast photoswitch, can be used as ligands that directly coordinate with iridium (III) ion. The iridium complexes show the characteristic photochromic reactions originating from the PIC moiety, whereas the behaviour of transient species is substantially different from that of PIC.

T-type photochromic reactions that are faster than second timescales are often called fast photochromism,[1,2] and have various potential applications beyond conventional photochromic compounds such as dynamic holographic materials,[3,4] anticounterfeiting materials, and nonlinear photofunctional materials that work with weak incoherent light.[5–7] Among several fast photochromic molecules reported so far, phenoxyl-imidazolyl radical complex (**PIC**) is one of the fast T-type photochromic compounds that form biradicals reversibly upon light irradiation (Scheme 1a).[8,9] **PIC** can be synthesised by simple synthetic procedures, and the photochromic reaction exhibits high fatigue resistance against repeated light irradiation. Furthermore, the thermal back reaction from the photogenerated open-ring isomer to the initial closed-ring isomer can be controlled from tens of nanoseconds to second timescales by rational design of the molecular framework. These characteristics are crucial for the abovementioned applications of fast photoswitch molecules. In addition, **PIC** has gained significant attention in biradical chemistry because metastable spin-correlated biradical species can be repeatedly generated by light irradiation.[10,11]

Scheme 1 Photochromic reaction schemes of (a) **PIC** and (b) **PIC**-coordinated iridium (III) complex derivatives.

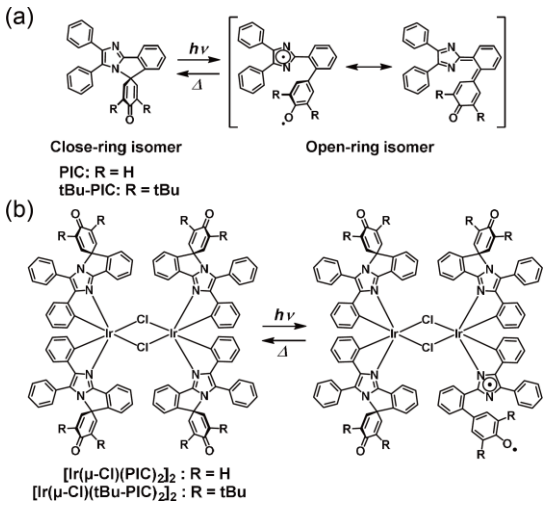

On one hand, **PIC** has a phenyl-imidazole moiety, which is often employed as a ligand for metal complexes.[12–14] Photochromic metal complexes exhibit several characteristic photofunctions such as the charge-transfer state between ligands and metal ions, and the enhanced spin-orbit interaction.[15–24] Moreover, the combination of photochromic molecules and multidentate ligands enables photochromic metal-organic frameworks that selectively capture guest molecules depending on light irradiation.[25] On the other hand, the photochromic metal complexes that have been reported so far are limited to P-type or slow T-type photochromic molecules. By combining metal complexes with fast photoswitches, advanced photofunctional materials can be developed such as visible-light-responsive fast photochromic molecules that can be synthesized only by coordination of fast photochromic molecules with metal ions, and nonlinear photochromic metal complexes that work under weak incident light.

[a] Department of Applied Chemistry, College of Life Sciences, Ritsumeikan University, Kusatsu, Shiga 525-8577, Japan. E-mail: ykobayas@fc.ritsumei.ac.jp; Tel: +81-77-561-3915
[b] Department of Chemistry and Biological Science, College of Science and Engineering, Aoyama Gakuin University, 5-10-1 Fuchinobe, Chuo-ku, Sagamihara, Kanagawa 252-5258, Japan. E-mail: jiro_abe@chem.aoyama.ac.jp; Tel: +81-42-759-6225
[c] Precursory Research for Embryonic Science and Technology (PRESTO), Science and Technology Agency (JST), 4-1-8 Honcho, Kawaguchi, Saitama 332-0012, Japan
Electronic Supplementary Information (ESI) available: CCDC 2245412 (**[Ir(μ-Cl)(PIC)$_2$]$_2$**) and 2245413 (**[Ir(μ-Cl)(tBu-PIC)$_2$]$_2$**). See DOI: 10.1039/x0xx00000x

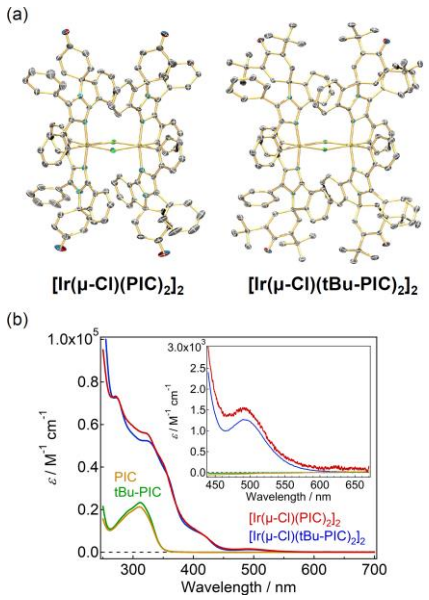

Fig. 1 (a) Crystal structures of **[Ir(μ-Cl)(PIC)$_2$]$_2$** and **[Ir(μ-Cl)(tBu-PIC)$_2$]$_2$**. (b) Steady-state absorption spectra of **[Ir(μ-Cl)(PIC)$_2$]$_2$**, **[Ir(μ-Cl)(tBu-PIC)$_2$]$_2$**, **PIC** and **tBu-PIC** in dichloromethane at room temperature. ε Indicates the molar absorption coefficients, and the inset shows the magnified spectra in the visible-light region.

In this study, we developed photochromic dinuclear iridium (III) (Ir^{3+}) complexes having **PIC** derivatives (**[Ir(μ-Cl)(PIC)$_2$]$_2$** and **[Ir(μ-Cl)(tBu-PIC)$_2$]$_2$**, Scheme 1b). We chose Ir^{3+} ion as a metal centre because it can be directly coordinated with the phenyl-imidazole moiety of **PIC**. Therefore, the photochromic reactions of the **PIC** units are expected to be altered largely by Ir^{3+} ions. We investigated the optical properties of these **[Ir(μ-Cl)(PIC)$_2$]$_2$** and **[Ir(μ-Cl)(tBu-PIC)$_2$]$_2$** by time-resolved visible and infrared (IR) spectroscopies ranging from sub-picosecond to milliseconds and density functional theory (DFT) calculations.

[Ir(μ-Cl)(PIC)$_2$]$_2$ and **[Ir(μ-Cl)(tBu-PIC)$_2$]$_2$** were synthesised by the reaction of $IrCl_3$•$n$$H_2O$ with the corresponding **PIC** derivatives in 1:2 stoichiometry. The resulting complexes were characterised by proton nuclear magnetic resonance (^{1}H NMR) spectroscopy, electrospray ionization (ESI) mass spectrometry, and single crystal X-rays crystallographic analyses (Fig. 1a and Fig. S1–S5 ESI†). Due to the difference in coordination structure, **[Ir(μ-Cl)(PIC)$_2$]$_2$** and **[Ir(μ-Cl)(tBu-PIC)$_2$]$_2$** have structural isomers (ΔΔ and ΛΛ forms). Single crystal X-ray diffraction analysis revealed that the ΔΔ and ΛΛ isomers are present in equal amounts in a crystal and that these complexes are racemic compounds (Fig. S6 and S7 ESI†). On the other hand, the diastereomer (ΔΛ form) was not observed probably due to steric hindrance between the **PIC** units. In subsequent spectroscopic measurements, these isomers were measured without optical resolution.

Fig. 1b shows the steady-state absorption spectra of the synthesised Ir^{3+} complexes and **PIC** derivatives in dichloromethane. **PIC** derivatives have absorption only shorter than 350 nm. The absorption spectrum of **PIC** is almost identical to that of **tBu-PIC**.[8] **[Ir(μ-Cl)(PIC)$_2$]$_2$** and **[Ir(μ-Cl)(tBu-PIC)$_2$]$_2$** are very similar to each other as similar to those of **PIC** and **tBu-PIC**. The absorption bands at ~340 nm of **[Ir(μ-Cl)(PIC)$_2$]$_2$** and **[Ir(μ-Cl)(tBu-PIC)$_2$]$_2$** are similar to those of **PIC** and **tBu-PIC** although the molar absorption coefficients are slightly lower than those of four times the values of **PIC** and **tBu-PIC** probably due to the spectral broadening. On the other hand, the Ir^{3+} complexes have additional absorption bands at 410 and 500 nm (inset of Fig 1b). DFT calculations with B3LYP/6-31G(C,H,O,N,Cl)/LANL2DZ(Ir) level of the theory suggest that these bands are ascribed to the metal-to-ligand charge transfer (MLCT) transitions (Fig. S23 and S24 ESI†).

To investigate the photochromic properties of **[Ir(μ-Cl)(PIC)$_2$]$_2$** and **[Ir(μ-Cl)(tBu-PIC)$_2$]$_2$**, laser flash photolysis measurements were performed using a 355-nm nanosecond laser pulse. The millisecond transient absorption spectra of **[Ir(μ-Cl)(PIC)$_2$]$_2$** in dichloromethane show a sharp absorption band at 360 nm, shoulder band at 410 nm, and broad absorption bands at ~520, 800, and 1400 nm immediately after the excitation (Fig. 2). These transient absorption bands are observed repeatedly. A reference compound that does not have photochromic units (**[Ir(μ-Cl)(2-phenylpyridine)$_2$]$_2$**, see Fig. S11 ESI† for the molecular structure), does not show any transient signals over milliseconds except for the slight photodegradation (Fig. S11 ESI†). These results suggest that the photochromic reaction of the **PIC** unit of **[Ir(μ-Cl)(PIC)$_2$]$_2$** proceeds as similar to

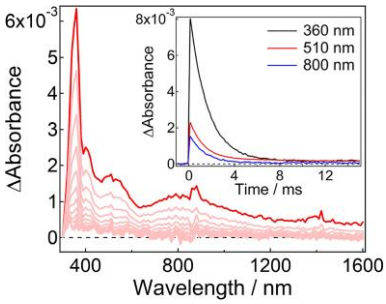

Fig. 2 Transient absorption spectra and (inset) dynamics of **[Ir(μ-Cl)(PIC)$_2$]$_2$** in dichloromethane (2.4×10^{-5} M) on sub-millisecond timescales excited with a 355-nm nanosecond laser pulse (1.0 mJ pulse^{-1}) under nitrogen atmosphere at room temperature.

PIC. This point is further elucidated by time-resolved IR spectroscopies as shown later. Moreover, the transient absorption dynamics are not affected by the presence of molecular oxygen (Fig. S8 ESI†). It suggests that the photochromic reaction of **[Ir(μ-Cl)(PIC)$_2$]$_2$** proceeds via the singlet excited state, i.e., the triplet excited state is not involved in the reaction in spite of the heavy metal complexes. All transient absorption bands of **[Ir(μ-Cl)(PIC)$_2$]$_2$** decay monotonically with a half-life of 1.5 ms (Fig. 2 inset), which is more than 2000 times longer than that of **PIC** (690 ns in dichloromethane at room temperature, Fig. S9 ESI†). Thermodynamic parameters for the thermal back reaction were obtained by the temperature dependence of the transient absorption dynamics (the details are shown in the ESI).

Because **[Ir(μ-Cl)(PIC)$_2$]$_2$** has four **PIC** units in a complex, it was initially expected that multiple open-ring isomers are

generated in a stepwise manner and intensity-dependent photochromic behaviours are observed. However, both experimental and theoretical calculations as explained below suggest that the photochromic reaction of **[Ir(μ-Cl)(PIC)$_2$]$_2$** involves the bond dissociation of only one **PIC** unit, instead of multiple **PIC** units. Transient absorption spectra and decay on millisecond timescales do not change at all even under intense excitation conditions (Fig. S13 ESI†). DFT calculations suggest that the absorption spectra of **[Ir(μ-Cl)(PIC)$_2$]$_2$** should change depending on the number of the open-ring isomer units (Fig. S25 ESI†). Moreover, the Gibbs free energies of **[Ir(μ-Cl)(PIC)$_2$]$_2$** are different depending on the number of open-ring isomer units. It indicates that the decay kinetics should change if multiple open-ring isomers are formed in **[Ir(μ-Cl)(PIC)$_2$]$_2$** (Fig. S26 ESI†). In addition, DFT calculations also suggest that the LUMO of **[Ir(μ-Cl)(PIC)$_2$]$_2$** having the open-ring isomer unit is localized at the open-ring isomer unit. It suggests that the open-ring isomer unit may suppress the stepwise photochromic reaction (Fig. S27 ESI†).

[Ir(μ-Cl)(tBu-PIC)$_2$]$_2$ does not show any transient absorption signals in the microsecond-to-millisecond timescales. In **tBu-PIC** (Scheme 1a), the rate of the thermal back reaction is greatly accelerated as compared to that of **PIC** due to the steric hindrance by the *tert*-butyl groups (Fig. S10 ESI†). Moreover, in the **PIC**-coordinated Ir^{3+} complexes, the coordination bonds between the Ir^{3+} ion and the **PIC** unit are expected to interfere with the structural change of the **PIC** unit after the bond breaking. These results suggest that the steric hindrance by *tert*-butyl groups and the coordination bonds with Ir^{3+} ion suppress the formation or largely destabilize the stable open-ring isomer of **[Ir(μ-Cl)(tBu-PIC)$_2$]$_2$**.

To further investigate the photochromic reactions of **[Ir(μ-Cl)(PIC)$_2$]$_2$** and **[Ir(μ-Cl)(tBu-PIC)$_2$]$_2$**, the transient absorption spectra from sub-picosecond to nanosecond were measured using a 347-nm excitation laser pulse. In **[Ir(μ-Cl)(PIC)$_2$]$_2$** in dichloromethane (Fig. 3a), sharp transient absorption bands at 465, 570 nm and a broad transient absorption band over visible to near-infrared light region are observed at 0.5 ps after the excitation. These transient absorption bands are tentatively ascribed to the S_1 state of the closed-ring isomer or the transient state just after the bond breaking. The transient absorption bands at 450–600 nm decay on a timescale of picoseconds, and another broad transient absorption band appears at 800 nm. The spectral shape does not change after 100 ps and is similar to that of the open-ring isomer observed on millisecond timescales. It indicates that the open-ring isomer is generated within tens of picoseconds. The signal decreases gradually on a timescale of nanoseconds (>10 ns). Actually, the decay of the transient signals is also observed until hundreds of nanoseconds in addition to the millisecond decay component (Fig. S8 ESI†). The fact that transient signals associated with the open-ring isomer are observed over millisecond timescales indicates that a portion of the open-ring isomer persists after its decay on nanosecond timescales. Detailed discussions of the decay are shown in the ESI.

Interestingly, the transient absorption spectra of **[Ir(μ-Cl)(tBu-PIC)$_2$]$_2$** in dichloromethane on sub-picosecond to nanosecond timescales are very similar to those of **[Ir(μ-Cl)(PIC)$_2$]$_2$** (Fig. 3b). It indicates that a similar photochromic reaction occurs in **[Ir(μ-Cl)(PIC)$_2$]$_2$** and **[Ir(μ-Cl)(tBu-PIC)$_2$]$_2$** on a timescale of nanoseconds. On the other hand, the relative amplitude of the open-ring isomer of **[Ir(μ-Cl)(tBu-PIC)$_2$]$_2$** is smaller than that of **[Ir(μ-Cl)(PIC)$_2$]$_2$**. Moreover, the open-ring isomer of **[Ir(μ-Cl)(tBu-PIC)$_2$]$_2$** decays faster than that of **[Ir(μ-Cl)(PIC)$_2$]$_2$**, and completely decays with a time constant of 3.0 ns (Fig. S12 ESI†). This result suggests that the nanosecond decay is probably due to the thermal back reaction of the open-ring isomer of **[Ir(μ-Cl)(tBu-PIC)$_2$]$_2$**. This result clearly shows the reason why **[Ir(μ-Cl)(tBu-PIC)$_2$]$_2$** does not show any signals on millisecond timescales.

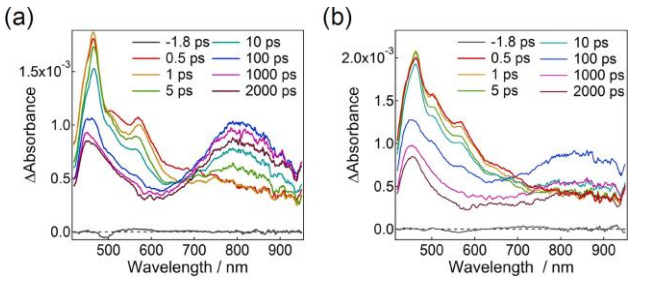

Fig. 3 Femtosecond to nanosecond transient absorption spectra of (a) **[Ir(μ-Cl)(PIC)$_2$]$_2$** and (b) **[Ir(μ-Cl)(tBu-PIC)$_2$]$_2$** in dichloromethane (1.2×10^{-4} and 1.5×10^{-4} M, respectively) excited at 347 nm (300 nJ pulse^{-1}) at room temperature.

The photochromic reaction of **[Ir(μ-Cl)(PIC)$_2$]$_2$** and **[Ir(μ-Cl)(tBu-PIC)$_2$]$_2$** can be also initiated by a 410-nm pulse, which selectively excites the MLCT band (Fig. S19 and S20 ESI†). However, since the absorption coefficient in the visible-light region is much smaller than that in the UV-light region, it is difficult to detect the transient signals of the open-ring isomer in the millisecond transient absorption measurements using a 532-nm nanosecond laser pulse.

To prove that the photochromic reactions of the **PIC**-coordinated Ir^{3+} complexes originate from the C–N bond dissociation of the **PIC** units, picosecond time-resolved IR spectra of **[Ir(μ-Cl)(PIC)$_2$]$_2$** and **[Ir(μ-Cl)(tBu-PIC)$_2$]$_2$** in deuterated dichloromethane were measured using a 355-nm femtosecond laser pulse as excitation pulse. Because the carbonyl group of the **PIC** moiety gives the intense and characteristic absorption band and the peak frequency of the carbonyl group is shifted depending on the radical property of the phenoxyl unit, the carbonyl group can be used as an efficient marker for the C–N bond dissociation of the **PIC** moiety.

In **[Ir(μ-Cl)(PIC)$_2$]$_2$** (Fig. 4a), broad featureless transient absorption bands are observed at ~1400, 1520, and >1660 cm^{-1} at 2 ps after the excitation. The broad absorption bands are probably assigned to the superposition of the S_1 state and the structurally unrelaxed biradical form formed just after the bond dissociation. Subsequently, these positive transient absorption bands gradually sharpened on a timescale of tens-to-hundreds of picoseconds, and distinct transient bands are observed at 1384, 1420, 1549, and 1584 cm^{-1}. Notably, the most intense

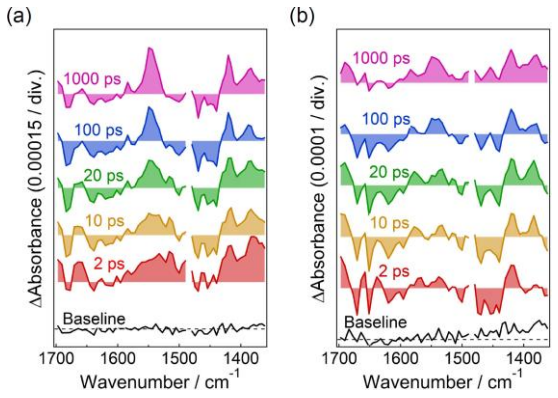

Fig. 4 Picosecond time-resolved IR spectra of (a) **[Ir(μ-Cl)(PIC)$_2$]$_2$** and (b) **[Ir(μ-Cl)(tBu-PIC)$_2$]$_2$** in deuterated dichloromethane (~5 × 10^{-3} M) excited with a 355-nm femtosecond laser pulse at room temperature.

band at 1549 cm^{-1} is well consistent with the stretching vibrational mode of the phenoxyl radical of the open-ring isomer of **PIC** in deuterated dichloromethane (Fig. S21 ESI†). **[Ir(μ-Cl)(tBu-PIC)$_2$]$_2$** also exhibits a similar signal at 1545 cm^{-1}, although the signals are smaller than those of **[Ir(μ-Cl)(PIC)$_2$]$_2$** probably due to the large steric hindrance (Fig 4b). It clearly indicates that the C–N bond of the **PIC** moiety was dissociated, and this reaction is the origin of the photochromic reaction of **[Ir(μ-Cl)(PIC)$_2$]$_2$** and **[Ir(μ-Cl)(tBu-PIC)$_2$]$_2$**. The time profile of the ground-state bleach signal at 1680 cm^{-1} gradually recovers on hundreds of picoseconds, which is qualitatively consistent with the transient absorption dynamics in the visible light region (Fig. S22 ESI†). On the other hand, the IR band at ~1550 cm^{-1} gradually increases on a timescale of hundreds of picoseconds. In **PIC** and pentaarylbiimidazole (**PABI**),[26] which is a derivative of **PIC**, the spin-spin interaction between two radicals dynamically evolved by rotation of the radical moieties on tens to hundreds of picoseconds after the bond dissociation. The gradual increase in the ~1550 cm^{-1} may indicate that the spin-spin interaction between the imidazolyl and phenoxyl radicals gradually increase on hundreds to picosecond timescales.

In conclusion, novel oxygen-independent photochromic Ir^{3+} complexes, **[Ir(μ-Cl)(PIC)$_2$]$_2$** and **[Ir(μ-Cl)(tBu-PIC)$_2$]$_2$**, were synthesised and their photochromic properties were investigated. The half-life of the thermal back reaction of **[Ir(μ-Cl)(PIC)$_2$]$_2$** is 1.5 ms, which is more than 2000 times longer than that of **PIC** used as a ligand. The combination of fast photoswitch molecules and metal complexes further expands the versatility of advanced photofunctional materials such as photoresponsive supramolecular radical cages[27,28] based on **PIC** framework.

This work was supported by JST, PRESTO Grant Numbers JPMJPR22N6, JSPS KAKENHI Grant Number JP18H05263, JP21K05012, The Murata Science Foundation, and Nippon Sheet Glass Foundation for Materials Science and Engineering. The computation was partially performed using the Research Center for Computational Science, Okazaki, Japan (Project: 22-IMS-C128).

Conflicts of interest

There are no conflicts to declare.

Notes and references

1. K. Fujita, S. Hatano, D. Kato and J. Abe, *Org. Lett.*, 2008, **10**, 3105–3108.
2. Y. Kishimoto and J. Abe, *J. Am. Chem. Soc.*, 2009, **131**, 4227–4229.
3. N. Ishii, T. Kato and J. Abe, *Sci. Rep.*, 2012, **2**, 819.
4. Y. Kobayashi and J. Abe, *Adv. Opt. Mater.*, 2016, **4**, 1354–1357.
5. Y. Kobayashi, K. Mutoh and J. Abe, *J. Phys. Chem. Lett.*, 2016, **7**, 3666–3675.
6. Y. Kobayashi, K. Mutoh and J. Abe, *J. Photochem. Photobiol., C*, 2018, **34**, 2–28.
7. Y. Kobayashi and J. Abe, *Chem. Soc. Rev.*, 2022, **51**, 2397–2415.
8. H. Yamashita, T. Ikezawa, Y. Kobayashi and J. Abe, *J. Am. Chem. Soc.*, 2015, **137**, 4952–4955.
9. T. Ikezawa, K. Mutoh, Y. Kobayashi and J. Abe, *Chem. Commun.*, 2016, **52**, 2465–2468.
10. K. Mutoh, S. Toshimitsu, Y. Kobayashi and J. Abe, *J. Am. Chem. Soc.*, 2021, **143**, 13917–13928.
11. M. Nishijima, K. Mutoh, R. Shimada, A. Sakamoto and J. Abe, *J. Am. Chem. Soc.*, 2022, **144**, 17186–17197.
12. E. Baranoff, S. Fantacci, F. De Angelis, X. Zhang, R. Scopelliti, M. Grätzel and M. K. Nazeeruddin, *Inorg. Chem.*, 2011, **50**, 451–462.
13. J. Ding, J. Gao, Y. Cheng, Z. Xie, L. Wang, D. Ma, X. Jing and F. Wang, *Adv. Funct. Mater.*, 2006, **16**, 575–581.
14. W. S. Huang, J. T. Lin, C. H. Chien, Y. T. Tao, S. S. Sun and Y. S. Wen, *Chem. Mater.*, 2004, **16**, 2480–2488.
15. C. C. Ko and V. W. W. Yam, *Acc. Chem. Res.*, 2018, **51**, 149–159.
16. C. L. Wong, M. Ng, E. Y. H. Hong, Y. C. Wong, M. Y. Chan and V. W. W. Yam, *J. Am. Chem. Soc.*, 2020, **142**, 12193–12206.
17. N. M. W. Wu, M. Ng and V. W. W. Yam, *Nat. Commun.*, 2022, **13**, 33.
18. A. Fernández-Acebes and J. M. Lehn, *Chem. Eur. J.*, 1999, **5**, 3285–3292.
19. V. Guerchais, L. Ordronneau and H. Le Bozec, *Coord. Chem. Rev.*, 2010, **254**, 2533–2545.
20. J. Boixel, V. Guerchais, H. Le Bozec, D. Jacquemin, A. Amar, A. Boucekkine, A. Colombo, C. Dragonetti, D. Marinotto, D. Roberto, S. Righetto and R. De Angelis, *J. Am. Chem. Soc.*, 2014, **136**, 5367–5375.
21. J. X. Wang, C. Li and H. Tian, *Coord. Chem. Rev.*, 2021, **427**, 213579.
22. L. A. Faustino, A. E. Hora Machado and A. O. T. Patrocinio, *Inorg. Chem.*, 2018, **57**, 2933–2941.
23. R. T. F. Jukes, B. Bozic, F. Hartl, P. Belser and L. De Cola, *Inorg. Chem.*, 2006, **45**, 8326–8341.
24. O. Galangau, L. Norel and S. Rigaut, *Dalton Trans.*, 2021, **50**, 17879–17891.
25. R. J. Li, J. Tessarolo, H. Lee and G. H. Clever, *J. Am. Chem. Soc.*, 2021, **143**, 3865–3873.
26. H. Yamashita, J. Abe, *Chem. Commun.*, 2014,**50**, 8468-8471.
27. K. Yazaki, S. Noda, Y. Tanaka, Y. Sei, M. Akita and M. Yoshizawa, *Angew. Chem. Int. Ed.*, 2016, **128**, 15255–15258.
28. B. Huang, L. Mao, X. Shi and H. B. Yang, *Chem. Sci.*, 2021, **12**, 13648–13663.